ASEC 2022

MDPI

*Proceeding Paper*

# Influence of the Characterization Methodology on the Repair Performance of Self-Healing Materials †

**J. Gómez-Sánchez *, A. Jiménez-Suárez, X. F. Sánchez-Romate and S. G. Prolongo**

Materials Science and Engineering Area, Escuela Superior de Ciencias Experimentales y Tecnología, Universidad Rey Juan Carlos, C/Tulipán s/n, 28933 Móstoles, Madrid, Spain; alberto.jimenez.suarez@urjc.es (A.J.-S.); xoan.fernandez.sanchezromate@urjc.es (X.F.S.-R.); silvia.gonzalez@urjc.es (S.G.P.)

* Correspondence: javier.gomez.sanchez@urjc.es

† Presented at the 3rd International Electronic Conference on Applied Sciences; Available online: https://asec2022.sciforum.net/.

**Abstract:** The repair performance of the so-called self-healing polymer systems has been extensively studied on recent works. However, the characterization methodology carried out to analyze the repair performance of these materials has not been widely discussed. Herein, a study of the influence of the characterization parameters on the self-healing capabilities of a 2-Aminophenyl disulfide (AFD)/epoxy system via convective heating is carried out. Results show a decrease of the self-healing efficiency proportional to the damage depth. Finally, increasing the healing temperature and time do not significantly affect the repair performance, obtaining similar self-healing efficiency values (>>95%) in all cases.

**Keywords:** self-healing; epoxy; AFD; vitrimer

**Citation:** Gómez-Sánchez, J.; Jiménez-Suárez, A.; Sánchez-Romate, X.F.; Prolongo, S.G. Influence of the Characterization Methodology on the Repair Performance of Self-Healing Materials. **2022**, *4*, x. https://doi.org/10.3390/xxxxx

Academic Editor(s):

Published: 1 December 2022

**Publisher's Note:** MDPI stays neutral with regard to jurisdictional claims in published maps and institutional affiliations.



## 1. Introduction

Covalent Adaptable Network (CAN) chemistry has been extensively introduced in thermoset resins to achieve self-healing properties. These polymers, also called vitrimers, are based on dynamic covalent bonds that break and re-form reversibly when subjected to an external stimulus, such as an increase of the temperature, pH variations, or UV radiation [1]. Among the different self-healing mechanisms, aromatic disulfide bridges have attracted much attention on recent works. These CANs are based on exchange reactions between adjacent S–S bonds that trigger a decrease of the viscosity, permitting the polymer gaining a high molecular mobility state and flow to recover from distortions, being able to restore the original properties of the material, i.e., self-healing [2].

Although repair phenomena of these systems have been demonstrated in previous investigations, the characterization methodology carried out to analyze the repair performance has not been widely discussed and generally provides a qualitative approach instead of quantitative results. Also, in other studies, the analysis of the self-healing efficiency consists of healing cracks from a scratched surface [3,4]. However, this kind of damage leads to material loss. Consequently, the restored material volume may not be the same as the original, so that the self-healing performance is expected to be degraded.

Moreover, the healing temperature is generally determined with the temperature at which disulfide exchange reactions occur, defined as the topology freezing transition temperature ($T_v$). However, for disulfide bond-based systems this temperature is below the

glass transition temperature ($T_g$), so that the exchange reactions occur at $T_v$, but the healing phenomenon is not achieved until reaching the $T_g$. This reaction is then governed by the viscosity of the resin, which drops above the $T_g$, following the Williams, Landel, and Ferry (WLF) model, and then decreases following the Arrhenius-type temperature dependence at higher temperatures [5]. The lower the viscosity the higher is the molecular mobility of the polymer network and, consequently, the repair performance may be increased. Furthermore, a longer healing time, defined as the relaxation time of the polymer above the $T_g$ [6], may permit the material to reach the healing temperature throughout its entire volume, thus increasing the self-healing efficiency. Therefore, the analysis of the effect of these parameters is of interest to define an optimal characterization of the self-healing capabilities in these systems.

In this regard, this research is focused on the study of the effect of the characterization methodology on the repair performance of self-healing materials. In this work, disulfide bonds were incorporated into an epoxy monomer with 2-Aminophenyl disulfide (AFD). The surface of the specimens was cut to generate cracks of different controlled depths and characterized with an optical profilometer. The effect of the damage dimensions, temperature and time on the self-healing capabilities of the AFD/epoxy system was studied.

## 2. Materials and Methods

### *2.1. Materials*

The epoxy resin was composed of Bisphenol A diglycidyl ether (DGEBA) and 2-Aminophenyl disulfide (AFD) hardener in different proportions: stoichiometric; R = 1.0, and with an AFD excess; R = 1.05, R = 1.1, R = 1.2, that is, with 5, 10% and 20% of AFD excess over the stochiometric proportion. Chemicals were supplied by Sigma-Aldrich and Tokyo Chemical Industry, respectively, and were used as received.

### *2.2. Manufacturing of 2-AFD/Epoxy Systems*

DGEBA monomer was first degassed during 15 min at 80 °C to remove the possible entrapped air. Then, the 2-AFD was added in a stoichiometric mass ratio of 100:36.5 (DGEBA:AFD; R = 1.0) and with 2-AFD excess (R = 1.05, R = 1.1 and R = 1.2) maintaining a temperature of 80 °C. The mixture was magnetically stirred for 5 min until phase miscibility occurred. Finally, it was poured into a metallic mold and cured at 160 °C for 6 h [7].

### *2.3. Thermomechanical Characterization*

Dynamic Mechanical Thermal Analysis (DMTA) measurements were performed following the ASTM 5418 in a Q800 DMA device, supplied by TA Instruments (New Castle, DE, USA). The tests were carried out in single cantilever mode with two specimens per condition, and the dimensions of the samples were 35 × 12.7 × 1.7 $mm^3$. They were subjected to a 2 °C/min heating rate from room temperature to 200 °C.

### *2.4. Self-Healing Tests*

Self-healing efficiencies were evaluated as a function of the crack depth, healing temperature, and healing time.

First, three cracks were induced on each sample by using a blade with a cutting edge forming 45°. On the one hand, three different depths were selected to analyze the influence of the crack depth on the self-healing performance of all the systems: 500 μm, 600 μm and 700 μm. Cracks with depths higher than 500 μm were cut with intermediate steps of 100 μm additional from the initial 500 μm, as shown in Table 1, since the blade flexed at higher depths and induced a heterogeneous crack.

**Table 1.** Crack generation procedure.

| Total Depth (μm) | Step 1 (μm) | Step 2 (μm) | Step 3 (μm) |
|---|---|---|---|

| | | | |
|---|---|---|---|
| 500 | 500 | - | - |
| 600 | 500 | 100 | - |
| 700 | 500 | 100 | 100 |

On the other hand, the analysis of the influence of the healing temperature and healing time were performed for three cracks with the optimum depth ($d_{optimum}$), where $d_{optimum}$ was defined as the depth value at which the highest self-healing efficiency was obtained.

After cracks were created, their topology was characterized by means of optical profilometry using a ZETA Z-20 optical profilometer from Zeta Inc. Instruments. For each crack, ten measurements were carried out by taking photograms of 900 × 1000 μm. In addition, a study of the influence of the profilometer on the measured volume was carried out (Figure S1 and Table S1, Supplementary Materials) in comparison with a Field Emission Gun—Scanning Electron Microscope (FEG-SEM, Nova NanoSEM FEI 230) to ensure that acceptable measurement tolerances were accomplished.

Samples were then subjected to convective thermal stimulus to reach the temperature at which the healing phenomenon triggers, which corresponds to the $T_g$, as stated before.

To analyze the self-healing capabilities as a function of the crack depth, AFD/epoxy systems were tested at $T_{g\text{-}min}$ + 80 °C, where $T_{g\text{-}min}$ was defined as the minimum glass transition temperature of all the systems. The healing time was set as 1.5 h, although other investigations show lower healing times associated to the relaxation time of the polymer networks [8]. These values were selected to guarantee that self-healing occurs in all cases.

Then, the influence of the temperature on the self-healing performance was characterized with three cracks of $d_{depth}$ at $T_{g\text{-}min}$, $T_{g\text{-}min}$ + 20 °C, $T_{g\text{-}min}$ + 40 °C and $T_{g\text{-}min}$ + 80 °C for 1.5 h. From the results of this analysis the optimum temperature ($T_{optimum}$) was defined as the temperature at which the highest self-healing efficiency was obtained. This temperature was applied as the self-healing temperature in the analysis of the effect of the healing time on the repair capacity. The study was performed for 0.5 h and 1.5 h.

The images taken by the profilometer were processed with an analysis software MountainsMap® to obtain the volumes of both the initial and healed cracks, and the self-healing efficiency, η, was defined as follows:

$$\eta(\%) = \frac{V_0 - V_f}{V_0} \times 100 \quad (1)$$

Where $V_0$ and $V_f$ were the initial and after healing volume of the crack, respectively.

## 3. Results and Discussion

### *3.1. Thermo-Mechanical Properties*

The healing temperature was determined from the $T_g$, which corresponds to the tan δ peak of the DMTA analysis. From the results shown in Table 2, it can be observed that an AFD excess content increases the number of reacted molecules, achieving a higher chemical conversion which leads to networks with a higher number of crosslinking points, reflected in an increase of the value of $T_g$. However, once surpassing a 10–20% of AFD excess a full chemical conversion of the epoxy groups is achieved but the presence of unreacted molecules increases. The preferential reaction of primary and secondary amine groups with respect of tertiary ones results in networks with higher molecular weight between crosslinks, which corresponds with a lower degree of crosslinking, thus a lower $T_g$ [9].

Since $T_{g\text{-}min}$ corresponds to the R = 1 and R = 1.2 systems, the healing temperature, which is $T_{g\text{-}min}$ + 80 °C as stated before, is set as 225 °C.

**Table 2.** Glass transition temperatures of the 2-AFD systems.

| AFD System | $T_g$ (°C) |
|---|---|
| R = 1.0 | 145.38 ± 0.32 |
| R = 1.05 | 151.72 ± 0.06 |

| | |
|---|---|
| R = 1.1 | 149.37 ± 0.73 |
| R = 1.2 | 144.17 ± 6.88 |

### *3.2. Influence of the Crack Depth*

From the self-healing efficiency results shown on Table 3 it can be observed that all AFD systems show similar values within a depth of 500 μm. However, the self-healing efficiency decreases with increasing the crack depth. The images of pre- and post-healing are shown in Figure S2. This phenomenon may be associated to the increase of material loss caused by the increasing blade cut steps, since each step drags an amount of scratched material. Consequently, the volume of the repaired crack decreases, thus the self-healing efficiency does.

**Table 3.** Self-healing efficiency of the AFD systems.

| AFD System | Self-Healing Efficiency (%) | | |
|---|---|---|---|
| | **500 μm** | **600 μm** | **700 μm** |
| R = 1.0 | 94.07 ± 1.55 | 88.24 ± 5.13 | NA |
| R = 1.05 | 96.81± 2.06 | 51.58 ± 9.39 | NA |
| R = 1.1 | 97.22 ± 1.46 | 86.12 ± 18.64 | NA |
| R = 1.2 | 96.58 ± 2.37 | 36.88 ± 45.88 | NA |

Moreover, the standard deviation of these results increases with the crack depth, as shown in Figure 1. Here, it can be observed that the measurements are not homogeneous and tend to show large variations depending on the measured region. These deviations may be given by the abovementioned drag of the scratched material with the cut blade.

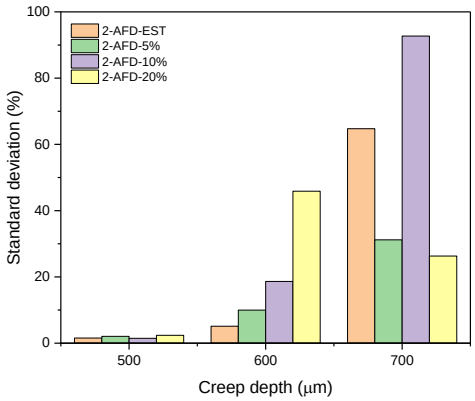


**Figure 1.** Standard deviation of the self-healing efficiency as a function of the crack depth.

This material is dragged not only being removed from the crack but also drawn towards the blade direction, being accumulated in other creep regions. These regions show higher self-healing efficiencies due to these material clusters, while in other zones the lack of material does not permit to fully fill the cavity and show lower self-healing efficiencies, being even not applicable as shown in Table 3. These NA values were discarded since the higher depth of the crack induced artifacts on the profilometer measurements which lead to volume values out of the mean of the set, thus obtaining high deviations on the results that did not permit calculating a consistent self-healing efficiency value.

Therefore, the optimum depth ($d_{optimum}$) is defined for a crack depth of 500 μm since it is associated to the highest self-healing efficiency values, as previously mentioned.

### *3.3. Influence of the Self-Healing Temperature*

After observing similar self-healing results for all the AFD contents on the system, the effect of the healing temperature and time will be studied only for the system with

DGEBA:AFD stoichiometric content (R = 1), since this condition proved enough healing efficiency and a reduced $T_g$ which leads to lower self-healing temperatures. Moreover, AFD excess could promote an early degradation of the material and the remaining unreacted molecules could migrate to the surface.

In this regard, once defined $d_{optimum}$, the influence of the healing temperature on the self-healing performance is analyzed. From the results shown in Table 4 it can be observed that all the experimental temperatures exhibit similar self-healing efficiency values, with very slight differences which are almost overshadowed by the standard deviations. This is explained because these experimental temperatures are higher than the $T_g$ of the stoichiometric system, thus the disulfide bond exchange reactions occur in all cases, as stated before. In addition, the self-healing efficiencies are so high that it is difficult to see any relevant differences. Therefore, it can be concluded that there is no significant influence of the healing temperature on the self-healing capacity of the AFD systems as long as this temperature is higher than the $T_g$.

**Table 4.** Self-healing efficiency as a function of temperature.

| AFD System | Temperature (°C) | η (%) |
|---|---|---|
| R = 1 | **140** | 98.83 ± 2.02 |
| | **160** | 98.26 ± 0.33 |
| | **180** | 96.9 ± 2.15 |
| | **220** | 94.07 ± 1.55 |

### *3.4. Influence of the Self-Healing Time*

Due to the similarity of the self-healing efficiencies as a function of the temperature, to proceed with the analysis of the influence of the healing time, $T_{optimum}$ is defined as the lowest temperature at which the repair phenomenon occurs, that is, T = 140 °C.

When observing the results shown in Figure 2, it can be realized that the self-healing efficiency values do not show a significant variation since the experimental time values are higher than the relaxation time of the polymer network defined in other studies [8] so that the disulfide exchange reactions occur within the established time range.

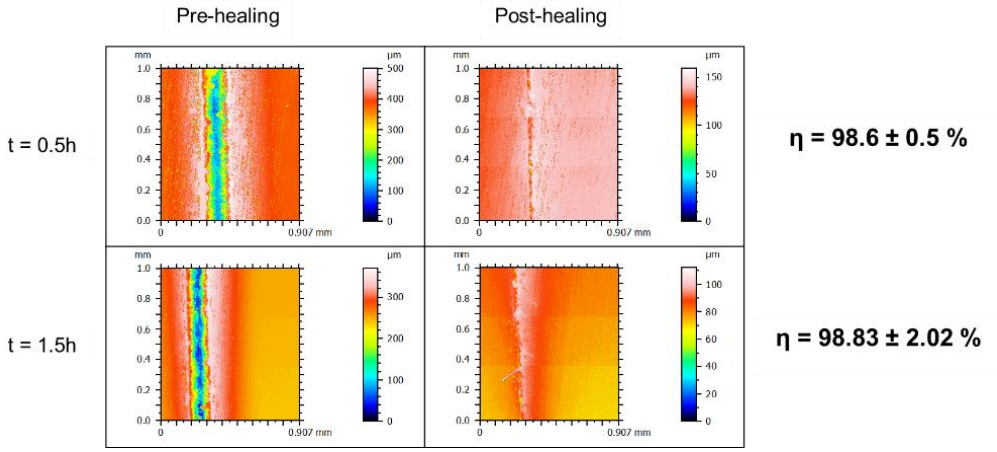


**Figure 2.** Self-healing efficiency as a function of time.

## 4. Conclusions

In this work, self-healing capabilities of AFD/epoxy systems were explored as a function of the main characterization parameters: crack depth, healing temperature and time.

The characterization methodology of the self-healing capabilities has been successfully implemented and validated for cracks with a 500 μm depth, which showed a similar healing efficiency for every AFD content, with values above 90% in every case indicating

an almost total recovery of the crack during the healing process. However, higher crack depths showed a detriment of the self-healing performance. This can be explained from the increase of material dragged by the blade on each cut step, which may be pulled out of the crack or even accumulated in other crack regions, causing a heterogeneous crack that, in addition to the artifacts detected by the profilometer at higher depths, do not provide consistent measurements of the crack volume.

Healing temperature and time did not show a significant variation of the self-healing efficiency since these experimental parameters were above the theoretical values at which the disulphide exchange reaction occurs.

Finally, it should be noted that the proposed experimental procedure, consisting of the combination of a controlled crack generation together with the evaluation of the cracks with an optical profilometer, has been successfully proven as an efficient quantitative method that reduces the uncertainty of the qualitative approaches presented in multiple published works.

**Supplementary Materials:** The following supporting information can be downloaded at: www.mdpi.com/xxx/s1, Figure S1: FEG-SEM characterization of the crack of the 2-AFD stoichiometric (R = 1) 0.2 wt.% CNT system with the (a) length and (b) volume measures.; Figure S2: Characterization of the 2-AFD stoichiometric (R = 1) system with the optical profilometer (a) pre- and (b) post-healing.; Table S1: Length and volume measures of the characterization methods.

**Author Contributions:** Conceptualization, A.J.-S. and S.G.P.; methodology, A.J.-S., X.F.S.-R. and J.G.-S.; validation, X.F.S.-R., and A.J.-S.; formal analysis, J.G.-S.; investigation, J.G.-S.; data curation, J.G.-S.; writing—original draft preparation, J.G.-S.; writing—review and editing, X.F.S.-R. and A.J.-S.; supervision, X.F.S.-R., A.J.-S. and S.G.P.; project administration, S.G.P. and A.J.-S.; funding acquisition, S.G.P. and A.J.-S. All authors have read and agreed to the published version of the manuscript.

**Funding:** This work was supported by the Agencia Estatal de Investigación of Spanish Government [PROJECT PID2019-106703RB-I00] and Young Reasearchers R&D Project [Ref. M2183, SMART-MULTICOAT] funded by Universidad Rey Juan Carlos and Comunidad de Madrid Regional Government.

**Institutional Review Board Statement:** Not applicable.

**Informed Consent Statement:** Informed consent was obtained from all subjects involved in the study.

**Data Availability Statement:** The data presented in this study are available on request from the corresponding authors.

**Conflicts of Interest:** The authors declare no conflict of interest.

## References

1. Yang, Y.; Ding, X.; Urban, M.W. Chemical and physical aspects of self-healing materials. *Prog. Polym. Sci.* **2015**, *49–50*, 34–59. https://doi.org/10.1016/j.progpolymsci.2015.06.001.
2. Islam, S.; Bhat, G. Progress and challenges in self-healing composite materials. *Mater. Adv.* **2021**, *2*, 1896–1926. https://doi.org/10.1039/d0ma00873g.
3. Amendola, E.; Iacono, S.d.; Pastore, A.; Curcio, M.; Iadonisi, A. Epoxy Thermosets with Self-Healing Ability. *J. Mater. Sci. Chem. Eng.* **2015**, *3*, 162–167. https://doi.org/10.4236/msce.2015.37022.
4. Bai, N.; Simon, G.P.; Saito, K. Characterisation of the thermal self-healing of a high crosslink density epoxy thermoset. *New J. Chem.* **2015**, *39*, 3497–3506. https://doi.org/10.1039/c5nj00066a.
5. van Zee, N.J.; Nicolaÿ R. Vitrimers: Permanently crosslinked polymers with dynamic network topology *Prog. Polym. Sci.* **2020,** *104*, 101233. https://doi.org/10.1016/j.progpolymsci.2020.101233.
6. de Luzuriaga, A.R.; Solera, G.; Azcarate-Ascasua, I.; Boucher, V.; Grande, H.J.; Rekondo, A. Chemical control of the aromatic disulfide exchange kinetics for tailor-made epoxy vitrimers. *Polymer* **2022**, *239*, 124457. https://doi.org/10.1016/j.polymer.2021.124457.
7. Martinez-Diaz, D.; Cortés, A.; Jiménez-Suárez, A.; Prolongo, S.G. Hardener Isomerism and Content of Dynamic Disulfide Bond Effect on Chemical Recycling of Epoxy Networks. *ACS Appl. Polym. Mater.* **2022**, *4*, 5068−5076. https://doi.org/10.1021/acsapm.2c00598.

8. de Luzuriaga, A.R.; Solera, G.; Azcarate-Ascasua, I.; Boucher, V.; Grande, H.J.; Rekondo, A. Chemical control of the aromatic disulfide exchange kinetics for tailor-made epoxy vitrimers. *Polymer* **2022**, *239*, 124457. https://doi.org/10.1016/j.polymer.2021.124457.
9. de Cárcer, I.A.; Prolongo, M.G.; Salom, C.; Parrado, J.; Moriche, R.; Prolongo, S.G. Thermal and Mechanical Properties of Self-Healing Epoxy/Graphene Nanocomposites. In Proceedings of the VIII ECCOMAS Thematic Conference on Smart Structures and Materials, Madrid, Spain, 5–8 June 2017; pp. 1399–1408.